Supporting Information

Predicted Polymorph Manipulation in Exotic Double Perovskite Oxide

He-Ping Su,[a] Shu-Fang Li,[b,*] Yi-Feng Han,[b] Mei-Xia Wu,[b] Churen Gui,[c] Yanfen Chang,[d] Mark Croft,[e] Steven Ehrlich,[f] Syed Khalid,[f] Umut Adem,[g] Shuai Dong,[c] Young Sun,[d] Feng Huang,[h] Man-Rong Li[b,*]

[a]School of Physics, Sun Yat-Sen University, Guangzhou 510275, P. R. China

[b]Key Laboratory of Bioinorganic and Synthetic Chemistry of Ministry of Education, School of Chemistry, Sun Yat-Sen University, Guangzhou 510275, P. R. China

[c]School of Physics, Southeast University, Nanjing 211189, China

[d]Beijing National Laboratory for Condensed Matter Physics, Institute of Physics, Chinese Academy of Sciences, Beijing 100190, P. R. China

[e]Department of Physics and Astronomy, Rutgers, The State University of New Jersey, Piscataway, NJ 08854, USA

[f]NSLS-II, Brookhaven National Laboratory, Upton, NY 11973, USA

[g]Department of Materials Science and Engineering, İzmir Institute of Technology, Urla 35430, İzmir, Turkey

[h]School of Materials, Sun Yat-Sen University, Guangzhou 510275, P. R. China

Email: limanrong@mail.sysu.edu.cn

Table of Contents

1. Experimental Procedures

1.1. Computational Descriptions.

To investigate the crystal structure evolution of MTO with increasing pressures, first-principles calculations based on density functional theory (DFT) were performed with the PBE-sol exchange correlation functional as implemented in Vienna *ab-initio* Simulation Package (VASP).[1, 2] The plane wave cutoff energy is set as 520 eV and the integrations in the Brillouin zone were performed with 4×4 ×3 γ-centered *k*-point mesh. Considering the strong correlation of the partially filled *d* shell of the Mn ion, an on-site Coulomb repulsion *U* was set using the Dudarev implementation.[3] Different *U* (3 and 4 eV) in the *R*-3 state have been tested for the *U*-dependence, which leads to a conclusion that $U = 3$ eV is the better choice. In fact, the results of different *U* shift insignificantly (**Table S1**). Different simplest ferromagnetic/antiferromagnetic order modes were adopted in all calculations by ignoring the energy shift that complex magnetic orders may lead to.

1.2 Synthesis.

Mg_3TeO_6-type MTO phase (rhombohedral *R*-3, denoted as AP-MTO) was synthesized by a conventional solid-state reaction using the following starting materials: MnO (99.99%, Alfa Aesar), Mn_2O_3 (99.99%, Sigma Aldrich), and TeO_2 (99.99%, Alfa Aesar). Stoichiometric mixtures of the starting materials were pelletized and heated in Ar at 1023 K for 24 h (heating and cooling rate of 5 K/min) with intermediate grinding as reported previously (**Fig. S1**).[4-7] Then the as-made AP-MTO precursor was loaded into a graphite heater lined with Pt capsule

inside an MgO crucible, followed by heating between 1173-1273 K at 5 GPa for 30 min in a Walker-type multi anvil press to prepare the HP phase (hereafter denoted as HP-MTO) as in our previous work.[8-14] Finally, the specimen was quenched to room temperature by tuning off the voltage supply to the resistance furnace. The pressure was maintained during the temperature quenching and slowly (typically within 8-12 h) decompressed to ambient.

1.3 Powder and Single Crystal X-ray Di□raction.

Both the AP and HP products were initially characterized by laboratory powder X-ray diffraction (PXD, Bruker D8 ADVANCE, Cu Kα, λ = 1.5418 Å) for phase identification and purity examination. Synchrotron powder X-ray di□raction (SPXD) data were collected at ambient condition on the beamline BL14B (λ = 0.68800 Å) at the Shanghai Synchrotron Radiation Facility (SSRF). The sample is loaded into a 0.5 mm glass capillary and the diffraction data were collected in spinning-mode. Mythen1K detector was used for high quality data acquisition and the wavelength (λ = 0.6895728 Å) was obtained using LaB_6 standard. The detailed information about beamline BL14B1 can be found in references.[15, 16] The SPXD data and crystal structure were analyzed and refined with the TOPAS-Academic V6 software package.[17] Single crystal of the HP-MTO was mounted on a glass fiber for single-crystal XRD analysis. The measurements were performed on a SuperNova di□ractometer equipped with graphite-monochromated Mo−$K\alpha$ radiation (λ = 0.71073 Å) at 293 K. The intensity data sets were collected with a ω-scan technique and reduced using CrystalClear software.[18] The structure of HP-MTO was computed through direct methods and refined using full-matrix least-squares techniques on F^2, with anisotropic thermal parameters for all atoms. All of the calculations were performed with the SHELXL 2013 package of crystallographic software.[19] The formulas collectively consider the crystallographically refined compositions and the requirements of charge neutrality.

1.4 X-ray Absorption Near Edge Spectroscopy.

Mn-K X-ray absorption near edge spectroscopy (XANES) data were collected in both the transmission and fluorescence mode with simultaneous standards. All of the spectra were fit to linear pre- and post-edge backgrounds and normalized to unity absorption edge step across the edge.[20-24] The title compound XANES spectra were collected at the QAS, 7BM Beamline at NSLS-II using a Si(111) channel-cut monochromator in the “quick”, continuous scanning mode. Some of the standard spectra were previously collected on beam line X-19A at NSLS-I with a Si-111 double crystal monochromator.

1.5 Magnetic and Magnetodielectric Properties Measurements.

Magnetization and magnetodielectric response were measured on a commercial Physical

Property Measurement System (PPMS). The magnetic susceptibility was measured in zero-field cooled (ZFC) and field cooled (FC) conditions under a 0.1 T magnetic field, for temperatures ranging from T = 5 to 300 K. Specific heat measurements between 10 and 60 K were also performed. To measure the dielectric constant, electrodes made of silver paste were painted on the widest faces of samples. The dielectric response was measured in a Cryogen-free Superconducting Magnet System (Oxford Instruments, Teslatron PT) using an LCR meter (Agilent E4980A) at frequencies of 1, 10, 100, and 1000 kHz.

2. Results and Discussion

2.1. Mn-K XANES.

XANES measurements of the K-edges of 3*d* row transition metals in compounds has proven to be a useful probe of the transition metal valence/configuration.[20-24] These edges are dominated by peak-like 1*s* to 4*p* transitions and typically exhibit a chemical shift to higher energies with increasing transition metal valance. Here the chemical shift can be monitored either by the energy of the peak or the rapidly-rising-portion of the near edge spectra. Referring to **Fig. S4a** the chemical shift of the peak-energy (indicated by the label "b") downward between $CaMn^{4+}O_3$, $LaMn^{3+}O_3$, and $Sr_2Mn^{2+}ReO_6$ standards is quite clear. The $Ba_2Mn^{2+}ReO_6$ spectrum illustrates how the main peak can be split into two components (b_1/b_2 in **Fig.S4a**), respectively shifted up (down) in energy but with the centrum of the split-peak feature lying in the Mn^{2+} energy range.[20, 22-24] A similar splitting is manifested in the $Mn^{2+}O$ spectrum.[23] Note also that the Mn^{2+} standard spectra also typically manifest a prominent a-feature (see **Fig. S4a** top) below the energy of the b-peak features.

The Mn-K main edges of HP-MTO and the isostructural Mn_2FeReO_6 are superimposed in **Fig. S4a**. It should be noted that the spectral peak of the Mn^{2+}, distorted perovskite-*A*-site, in the latter spectrum, is noticeably shifted to lower energy (see line "2" in figure) relative to the peaks in the other Mn^{2+} spectra,[24] but is still consistent with the divalent assignment. The HP-MTO spectrum is consistent with two Mn^{2+}, *A*-sites, similar to Mn_2FeReO_6, and one Mn^{2+} *B*-site, similar to $Ba_2Mn^{2+}ReO_6$. Specifically, the Mn^{2+} *B*-site contributes the following spectral features: the sharp, split b1/b2 peaks at the vertical lines labeled 2/3; and the clear excess intensity at the position labeled by the 1-line which falls at the energy expected for an a-feature (noted above). Note that both the A-site and B-site make contributions in the vicinity of the line labeled 1 in the figure.

The pre-edge portion of the Mn-K spectra are shown in **Fig. S4b**. Such pre-edge spectral features involve quadrupole, and d/p-hybridization induced dipole, transitions into final *d*-

states.[21, 24] Again, an increasing-valence/chemical-shift-to-higher-energy is typically seen in the pre-edge features, along with changes in the spectral distribution. Comparison of the HP-MTO pre-edge feature to those of the standard compounds further supports the Mn^{2+} assignment for this compound. Thus, both the main-edge and pre-edge Mn K results support a Mn^{2+} state for the *A*- and *B*- sites in HP-MTO.

2.2. Polymorphs of $A_2BB'O_6$ with small A-site cations.

$A_2BB'O_6$ compounds with small *A*-site cation, where the ionic radius of *A* is no larger than that of the high spin (HS) Mn^{2+}, can adopt a number of structure types.[25-29] These are distorted $GdFeO_3$-derived (monoclinic $P2_1/n$) double perovskite, corundum derivatives ($LiNbO_3$-type $R3c$, ilmenite $R\bar{3}$, ordered ilmenite, or Ni_3TeO_6 type $R3$), $LiSbO_3$ derivatives (*B*-site ordered, *Pnn*2), Mg_3TeO_6 ($R\bar{3}$), bixbyite ($Ia\bar{3}$), and β-Li_3VF_6 ($C2/c$) as shown in **Fig. 1**. So far, the well-known double-perovskites (AO_8 in framework of rock-salt ordering BO_6 and $B'O_6$) have only been reported in $Mn_2BB'O_6$ (*B* = Sc,[30] V,[31] Cr,[32] Mn,[9, 33] Fe,[10, 34-37] *B*' = Sb,[30-32, 34-36] Re;[9, 10, 33, 37] and *B* = $Fe_{0.8}Mo_{0.2}$,[38] *B*' = Mo[38]). The corundum family can be described as highly perovskite-related structure considering the very similar BO_6 and $B'O_6$ arrangement, regardless of their face-sharing AO_6 counterparts.[26] Their crystal structures are mainly dependent on the cationic ordering degree over the *B* and *B*' sites,[39] giving $LiNbO_3$ ($R3c$) or ilmenite ($R\bar{3}$) type structure with disordered *B*/*B*', or ordered ilmenite ($R3$) or Ni_3TeO_6 ($R3$) symmetry with ordered arrangement of *B* and *B*'. So far, Li^+, Mn^{2+}, Ni^{2+}, and Zn^{2+} have been predicted or incorporated into the *A*-sites of corundum derivatives in Li_2BTeO_6 (*B* = Ge,[40] Zr, Hf[41]), $Mn_2BB'O_6$ (*B* = Mn,[42] Fe,[11, 13, 14, 43, 44] In,[45] *B*' = Sb,[43, 45] Nb,[14] Ta,[14] Mo,[13, 44] W[11, 42]), $Ni_2BB'O_6$ (*B* = Ni,[46] Sc, [47] In, [47] *B*' = Sb, [47] Te[46]), and $Zn_2FeB'O_6$ (*B*' = Ta,[12] Os[48]). The $LiSbO_3$ derived Li_2BTeO_6 (*B* = Ge,[49] Ti,[50] Sn[50]) possess edge-sharing octahedral chains of alternatively ordered BO_6 and TeO_6 with two distinct 6-folded Li atoms zigzagged down the channels. The Mg_3TeO_6-type A_3TeO_6 (*A* = *B* = Mg,[51-55] Mn[4-7, 56]), Mn_2BSbO_6 (*B* = Sc, In),[57] and Sc_3CrO_6[58] have octahedral coordination of all the cation sites with the *A* and *B* cations are fully disordered, as also appears in bixbyite-type $Cu_2BB'O_6$ (*B* = Ga, Mn, Fe, *B*' = Sb;[59] *B* = Co,[60] Ni,[61] Cu,[5, 62-70] *B*' = Te), $In_2RuB'O_6$ (*B*' = Mn, Fe),[71] and Hg_3TeO_6,[72] in which $(A_{2/3}B_{1/3})O_6$ and $B'O_6$ are connected via edge-sharing.[72] The β-Li_3VF_6 structural A_3TeO_6 (*A* = Co,[4-6, 73-81] Zn[82]) are not so common and have the richest cationic arrangement with the coexistence of AO_4, AO_5, AO_6, and TeO_6. The aforementioned diversity of potential structure types of these $A_2BB'O_6$ compounds makes it a challenge to design and identify desired multifunctional materials. Empirically, in $LiSbO_3$-derived *Pnn*2 type structure, the charge differences between *B* and *B*' site is no more than 2 in the known compound, while in In bixbyite $Ia\bar{3}$ structure, the ionic size difference

between cations is usually no larger than 0.2 Å. The coexistenc of three, four, five and six coordination in β-Li_3VF_6 structure does not favor large ionic radius, especially for the five-coordinated site, the ionic radius is no more than 0.7 Å in known materials. Therefore, chemically and geometrically view, $Mn^{2+}{}_2Mn^{2+}Te^{6+}O_6$ does not favor the formation of bixbyite *Ia*-3, $LiSbO_3$-derived *Pnn*2, or β-Li_3VF_6-type *C*2/*c* structure type.

3. Graphics and Supporting Data

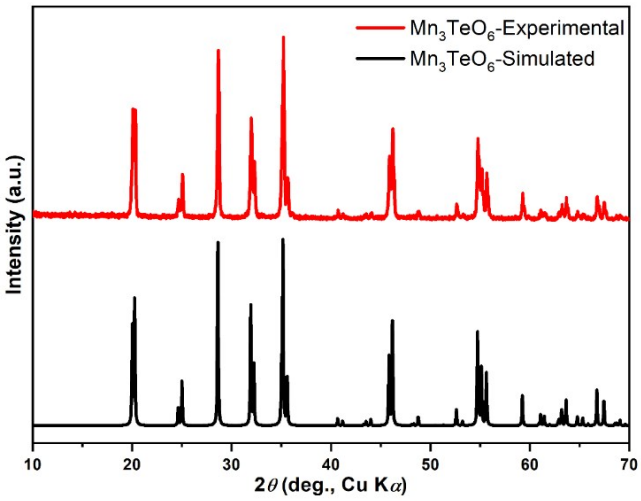

Fig. S1 Experimental (top) and simulated (bottom) XRD patterns of the AP-Mn_3TeO_6, showing typical Mg_3TeO_6-type (*R*-3) phase.

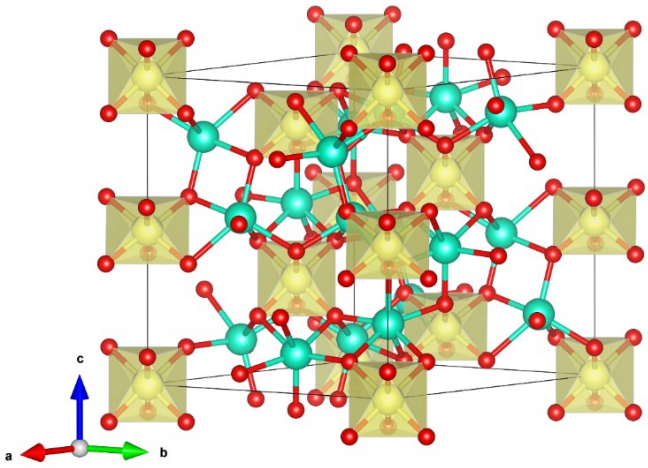

Fig. S2 Polyhedral viewing of the crystal structure of AP-Mn_3TeO_6, which is isotypic with Mg_3TeO_6 and can be derived from close packing of strongly distorted hexagonal oxygen layers parallel to (001), with Mn and two distinct Te atoms in the octahedral interstices. The TeO_6 octahedra are very regular, with 3 symmetry, whereas the MnO_6 octahedra are considerably distorted. Both TeO_6 octahedra are isolated and share edges with six MnO_6 octahedra of edge-sharing MnO_6 pairs. Mn, cyan spheres; O, red spheres; TeO_6, yellow.

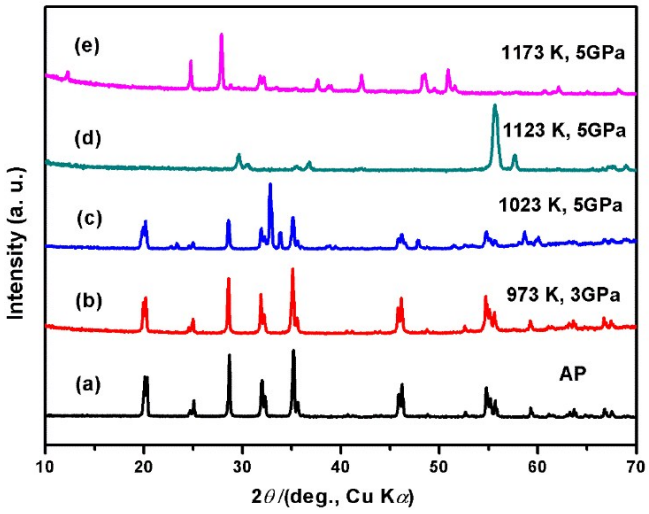

Fig. S3 Comparison of the PXD patterns of (a) AP-Mn_3TeO_6 and after treated at (b) 973 K and 3 GPa, (c) 1023 K and 5 GPa, (d) 1123 K and 5 GPa, and (e) 1173 K and 5 GPa.

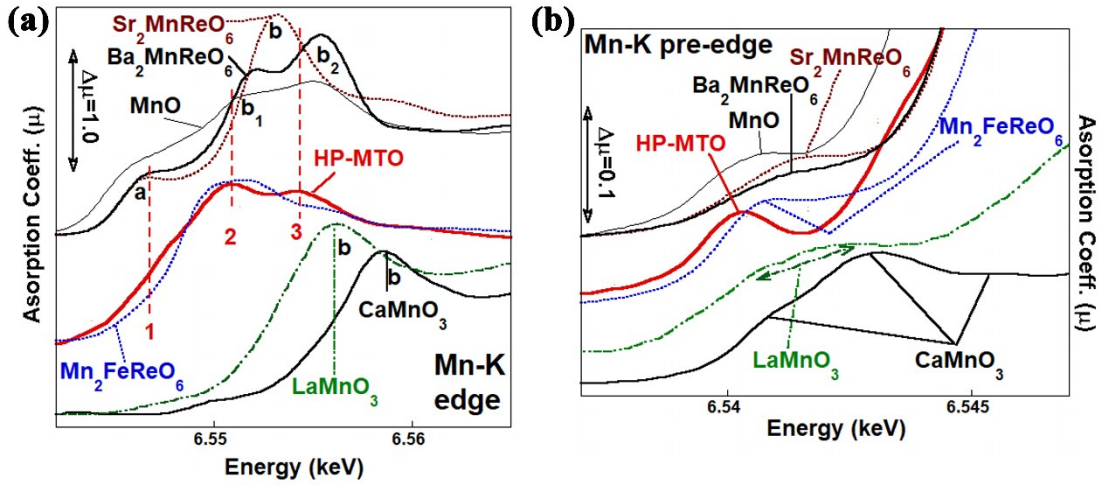

Fig. S4 (a) The Mn-K main-edge of HP-MTO is compared to the edges of a series of standard compounds with differing formal valence states and local coordination. The overlaid $Mn^{2+}{}_2FeReO_6$ spectrum has Mn in highly distorted perovskite-*A*-sites with coordination reduced to eight-fold (with four short and four long bonds) similar to two of the sites in the title compound. For clarity, the following octahedrally coordinated standard spectra are presented vertically displaced upward (downward) for Mn^{2+} (Mn^{3+}) standards: $Mn^{2+}O$ (with edge sharing); the B-site (corner sharing) perovskite based $CaMn^{4+}O_3$, $LaMn^{3+}O_3$, $Sr_2Mn^{2+}ReO_6$, and $Ba_2Mn^{2+}ReO_6$. Note that the local maximum peaks of the spectra have been labeled b (or b1/b2 in the cases where a split-peak occurs). A prominent lower energy shoulder in the Mn^{2+} standards is also labeled "a". (b) The Mn-K pre-edge of HP-MTO compared to the same series of standard compounds as in the previous figure. Again, vertical displacement for clarity is used.

Table S1. Comparison of the lattice parameters, magnetic moment, and gap at experimental and different *U* values for calculations.

	experimental	$U = 3$ eV	$U = 4$ eV
a (Å)	8.8675	8.8809	8.8954
b (Å)	8.8675	8.8809	8.8954
c (Å)	10.6731	10.7138	10.714
Moment (μ_B/Mn)		4.578	4.615
Gap (meV)		~536	~665

Table S2. Structure parameters for HP-MTO at room temperature refined using SPXD and single crystal data, respectively.

Atom	Site	*Occ.*	*x*	*y*	*z*	*B*/Å^2
SPXD						
Mn1	4*e*	1.0	0.0107(1)	0.0475(1)	0.2406(1)	1.230(1)
Mn2	2*c*	1.0	0	0.5	0	0.889(1)
Te1	2*d*	1.0	0.5	0	0	0.761(1)
O1	4*e*	1.0	0.3382(1)	0.3018(1)	0.0831(1)	1.048(1)
O2	4*e*	1.0	0.1946(1)	0.8242(1)	0.0463(1)	1.048(1)
O3	4*e*	1.0	-0.1308(1)	0.4302(1)	0.2706(1)	1.048(1)
Monoclinic space group $P2_1/n$ (No.14), $a = 5.2945(1)$ Å, $b = 5.4527(1)$ Å, $c = 7.8092(1)$ Å, $\beta = 90.37(1)°$, $V = 225.44$ (1) Å^3, $Z = 2$, $R_{wp} = 9.96\%$, $R_p = 6.50\%$.						
Single crystal						
Mn1	4*e*	1.0	0.0119(1)	0.9530(2)	0.2399(1)	0.05(1)
Mn2	2*c*	1.0	0	0.5	0.	0.04(1)
Te1	2*d*	1.0	0	0.5	0.5	0.03(1)
O1	4*e*	1.0	0.1669(5)	0.2103(5)	0.4178(3)	0.07(1)
O2	4*e*	1.0	0.3007(5)	0.6779(5)	0.4481(3)	0.09(1)
O3	4*e*	1.0	0.1268(5)	0.4240(5)	0.7276(3)	0.05(1)
Monoclinic space group $P2_1/n$ (No.14), $Z = 2$, $a = 5.286(1)$ Å, $b = 5.448(1)$ Å, $c = 7.797(1)$ Å, $\beta = 90.37(1)°$, $V = 224.51$ (1)Å^3, $R_1 = 1.69$ %, $R_2 = 1.90$ %.						

Table S3. Selected interatomic distances (Å), bond angles (°) and atomic BVS in HP-MTO at room temperature using SPXD and single crystal data, respectively.

SPXD			
Mn1−O1	2.077(1)	Mn2−O2 (×2)	2.077(1)
Mn1−O3	2.112(1)	Mn2−O3 (×2)	2.187(1)
Mn1−O2	2.180(1)	Mn2−O2 (×2)	2.261(1)
Mn1−O3	2.230(1)	(Mn2−O)	2.175(1)
Mn1−O1	2.544(1)	BVS	2.16
Mn1−O2	2.581(1)	Te1−O2 (×2)	1.916(1)
Mn1−O2	2.728(1)	Te1−O3 (×2)	1.953(1)
Mn1−O1	2.948(1)	Te1−O1 (×2)	1.967(1)
(Mn−O)	2.425(1)	(Te−O)	1.946(1)
BVS	1.90	BVS	5.56
Single Crystal			
Mn1−O1	2.132(3)	Mn2−O2 (×2)	2.085(3)
Mn1−O3	2.144(3)	Mn2−O1(×2)	2.193(3)
Mn1−O2	2.157(3)	Mn2−O3(×2)	2.269(2)
Mn1−O3	2.196(3)	(Mn2−O)	2.182
Mn1−O1	2.484(3)	BVS	2.122
Mn1−O2	2.626(3)	Te1−O2 (×2)	1.907(3)
Mn1−O2	2.679(3)	Te1−O1 (×2)	1.920(3)
Mn1−O2	2.805(3)	Te1−O3 (×2)	1.938(3)
(Mn−O)	2.403	(Te−O)	1.922
BVS	1.898	BVS	5.928

4. References

1. A. R. J. P. Perdew, G. I. Csonka, O. A. Vydrov, G. E. Scuseria, L. A. Constantin, X. Zhou, and K. Burke, *Phys. Rev. Lett.*, 2007, 136406.
2. A. R. J. P. Perdew, G. I. Csonka, O. A. Vydrov, G. E. Scuseria, L. A. Constantin, X. Zhou, and K. Burke, 2009, **102**, 39902.
3. G. A. B. S. L. Dudarev, S. Y. Savrasov, C.J. Humphreys, and A.P. Sutton, *Phys. Rev. B- Condens. Matter Mater. Phys*, 1998, **57**, 1505.
4. N. V. Golubko, V. Y. Proidakova, G. M. Kaleva, S. A. Ivanov, A. V. Mosunov, S. Y. Stefanovich, N. V. Sadovskaya, E. D. Politova and P. Nordblad, *Bull. Russ. Acad. Sci. Phys*, 2010, **74**, 724-726.
5. R. Mathieu, S. A. Ivanov, P. Nordblad and M. Weil, *Eur. Phys. J. B*, 2013, **86**, 1-4.
6. H. Singh, A. K. Sinha, H. Ghosh, M. N. Singh, P. Rajput, C. L. Prajapat, M. R. Singh and G. Ravikumar, *J. Appl. Phys.*, 2014, **116**, 074904-074901-074904-074909.
7. M. Weil, *Acta Crystallogr. Sec. E*, 2006, **62**, i244-i245.

8. M.-R. Li, M. Retuerto, P. W. Stephens, M. Croft, D. Sheptyakov, V. Pomjakushin, Z. Deng, H. Akamatsu, V. Gopalan, J. Sánchez-Benítez, F. O. Saouma, J. I. Jang, D. Walker and M. Greenblatt, *Angew. Chem. Int. Ed.*, 2016, **55**, 9862-9867.
9. M.-R. Li, J. P. Hodges, M. Retuerto, Z. Deng, P. W. Stephens, M. C. Croft, X. Deng, G. Kotliar, J. Sánchez-Benítez, D. Walker and M. Greenblatt, *Chem. Mater.*, 2016, **28**, 3148-3158.
10. M.-R. Li, M. Retuerto, Z. Deng, P. W. Stephens, M. Croft, Q. Huang, H. Wu, X. Deng, G. Kotliar, J. Sánchez-Benítez, J. Hadermann, D. Walker and M. Greenblatt, *Angew. Chem. Int. Ed.*, 2015, **54**, 12069-12073.
11. M.-R. Li, M. Croft, P. W. Stephens, M. Ye, D. Vanderbilt, M. Retuerto, Z. Deng, C. P. Grams, J. Hemberger, J. Hadermann, W.-M. Li, C.-Q. Jin, F. O. Saouma, J. I. Jang, H. Akamatsu, V. Gopalan, D. Walker and M. Greenblatt, *Adv. Mater.*, 2015, **27**, 2177-2181.
12. M.-R. Li, P. W. Stephens, M. Retuerto, T. Sarkar, C. P. Grams, J. Hemberger, M. C. Croft, D. Walker and M. Greenblatt, *J. Am. Chem.Soc.*, 2014, **136**, 8508-8511.
13. M.-R. Li, M. Retuerto, D. Walker, T. Sarkar, P. W. Stephens, S. Mukherjee, T. S. Dasgupta, J. P. Hodges, M. Croft, C. P. Grams, J. Hemberger, J. Sánchez-Benítez, A. Huq, F. O. Saouma, J. I. Jang and M. Greenblatt, *Angew. Chem. Int. Ed.*, 2014, **53**, 10774-10778.
14. M.-R. Li, D. Walker, M. Retuerto, T. Sarkar, J. Hadermann, P. W. Stephens, M. Croft, A. Ignatov, C. P. Grams, J. Hemberger, I. Nowik, P. S. Halasyamani, T. T. Tran, S. Mukherjee, T. S. Dasgupta and M. Greenblatt, *Angew. Chem. Int. Ed.*, 2013, **52**, 8406-8410.
15. T.-Y. Yang, W. Wen, G.-Z. Yin, X.-L. Li, M. Gao, Y.-L. Gu, L. Li, Y. Liu, H. Lin, X.-M. Zhang, B. Zhao, T.-K. Liu, Y.-G. Yang, Z. Li, X.-T. Zhou and X.-Y. Gao, *Nucl. Sci. Tech.*, 2015, **26**, 020101.
16. M. Gao, Y. L. Gu, L. Li, Z. L. Gong, X. Y. Gao and W. Wen, *J. Appl. Crystallogr.*, 2016, **49**, 1182-1189.
17. A. Coelho, *J. Appl. Crystallogr.*, 2000, **33**, 899-908.
18. Rigaku, 1.3.5 ed., Rigaku Corp., Tokyo, **2002**
19. G. Sheldrick, *Acta Crystallogr., Sect. A: Found. Adv.* 2015, **71**, 3-8.
20. T. K. Mandal, M. Croft, J. Hadermann, G. Van Tendeloo, P. W. Stephens and M. Greenblatt, *J. Mater. Chem.*, 2009, **19**, 4382-4390.
21. M. Croft, D. Sills, M. Greenblatt, C. Lee, S. W. Cheong, K. V. Ramanujachary and D. Tran, *Phys. Rev. B (Condensed Matter)*, 1997, **55**, 8726-8732.
22. G. Popov, M. Greenblatt and M. Croft, *Phys. Rev. B*, 2003, **67**, 024406.
23. Q. S. Lin, M. Greenblatt and M. Croft, *J. Solid State Chem.*, 2005, **178**, 1356-1366.
24. M. R. Li, M. Retuerto, Z. Deng, P. W. Stephens, M. Croft, Q. Z. Huang, H. Wu, X. Y. Deng, G. Kotliar, J. Sanchez-Benitez, J. Hadermann, D. Walker and M. Greenblatt, *Angew. Chem. Int. Ed.*, 2015, **54**, 12069-12073.
25. D. M. Giaquinta and H.-C. zur Loye, *Chem. Mater.*, 1994, **6**, 365-372.
26. A. Navrotsky, *Chem. Mater.*, 1998, **10**, 2787-2793.
27. S. Vasala and M. Karppinen, *Prog. Solid State Ch.*, 2015, **43**, 1-36.
28. A. Hossain, P. Bandyopadhyay and S. Roy, *J. Alloys Compd.*, 2018, **740**, 414-427.
29. A. B. Alexei and Y. Wei, *J. Phy.: Condens. Matter*, 2014, **26**, 163201.
30. E. Solana-Madruga, A. J. Dos santos-Garcia, A. M. Arevalo-Lopez, D. Avila-Brande, C. Ritter, J. P. Attfield and R. Saez-Puche, *Dalton Trans.*, 2015, **44**, 20441-20448.
31. G. V. Bazuev, A. P. Tyutyunnik, M. V. Kuznetsov and Y. G. Zainulin, *J. Supercond. Nov. Magn.*, 2018, **31**, 2907-2914.

32. A. J. Dos santos-Garcia, E. Solana-Madruga, C. Ritter, D. Avila-Brande, O. Fabelo and R. Saez-Puche, *Dalton Trans.*, 2015, **44**, 10665-10672.
33. A. M. Arevalo-Lopez, F. Stegemann and J. P. Attfield, *Chem. Commun.*, 2016, **52**, 5558-5560.
34. A. J. D. Santos-García, C. Ritter, E. Solana-Madruga and R. Sáez-Puche, *J. Phy.: Condens. Matter*, 2013, **25**, 206004.
35. R. Mathieu, S. A. Ivanov, I. V. Solovyev, G. V. Bazuev, P. Anil Kumar, P. Lazor and P. Nordblad, *Phys. Rev. B*, 2013, **87**, 014408.
36. A. P. Tyutyunnik, G. V. Bazuev, M. V. Kuznetsov and Y. G. Zainulin, *Mater. Res. Bull.*, 2011, **46**, 1247-1251.
37. A. M. Arévalo-López, G. M. McNally and J. P. Attfield, *Angew. Chem. Int. Ed.*, 2015, **54**, 12074-12077.
38. M.-R. Li, P. W. Stephens, M. Croft, Z. Deng, W. Li, C. Jin, M. Retuerto, J. P. Hodges, C. E. Frank, M. Wu, D. Walker and M. Greenblatt, *Chem. Mater.*, 2018, **30**, 4508-4514.
39. G.-H. Cai, M. Greenblatt and M.-R. Li, *Chem. Mater.*, 2017, **29**, 5447-5457.
40. P. M. Woodward, A. W. Sleight, L.-S. Du and C. P. Grey, *J. Solid State Chem.*, 1999, **147**, 99-116.
41. J. Choisnet, A. Rulmont and P. Tarte, *J.Solid State Chem.*, 1988, **75**, 124-135.
42. M.-R. Li, E. E. McCabe, P. W. Stephens, M. Croft, L. Collins, S. V. Kalinin, Z. Deng, M. Retuerto, A. Sen Gupta, H. Padmanabhan, V. Gopalan, C. P. Grams, J. Hemberger, F. Orlandi, P. Manuel, W.-M. Li, C.-Q. Jin, D. Walker and M. Greenblatt, *Nat. Commun.*, 2017, **8**, 2037.
43. A. J. Dos santos-García, E. Solana-Madruga, C. Ritter, A. Andrada-Chacón, J. Sánchez-Benítez, F. J. Mompean, M. Garcia-Hernandez, R. Sáez-Puche and R. Schmidt, *Angew. Chem. Int. Ed.*, 2017, **56**, 4438-4442.
44. Z.-J. Zhang, T.-T. Jin, M.-M. Xu, Q.-Z. Huang, M.-R. Li and J.-T. Zhao, *Inorg. Chem.*, 2015, **54**, 969-975.
45. Á. M. Arévalo-López, E. Solana-Madruga, E. P. Arévalo-López, D. Khalyavin, M. Kepa, A. J. Dos santos-García, R. Sáez-Puche and J. P. Attfield, *Phys. Rev. B*, 2018, **98**, 214403.
46. Y. S. Oh, S. Artyukhin, J. J. Yang, V. Zapf, J. W. Kim, D. Vanderbilt and S.-W. Cheong, *Nat. Commun.*, 2014, **5**.
47. S. A. Ivanov, R. Mathieu, P. Nordblad, R. Tellgren, C. Ritter, E. Politova, G. Kaleva, A. Mosunov, S. Stefanovich and M. Weil, *Chem. Mater.*, 2013, **25**, 935-945.
48. P. S. Wang, W. Ren, L. Bellaiche and H. J. Xiang, *Phys. Rev. Lett.*, 2015, **114**, 147204.
49. M.-H. Zhao, W. Wang, Y. Han, X. Xu, Z. Sheng, Y. Wang, M. Wu, C. P. Grams, J. Hemberger, D. Walker, M. Greenblatt and M.-R. Li, *Inorg. Chem.*, 2019, **58**, 1599-1606.
50. J. Choisnet, A. Rulmont and P. Tarte, *J. Solid State Chem.*, 1989, **82**, 272-278.
51. H. Schulz and G. Bayer, *Acta Crystallogr. Sec. B*, 1971, **27**, 815-821.
52. G. Blasse and W. Hordijk, *J. Solid State Chem.*, 1972, **5**, 395-397.
53. R. E. Newnham, J. F. Dorrian and E. P. Meagher, *Mater. Res. Bull.*, 1970, **5**, 199-202.
54. H. Schulz and G. Bayer, *Naturwissenschaften*, 1970, **57**, 393-393.
55. H. Kasper, *Z. Anorg. Allg. Chem.*, 1968, **356**, 329-336.
56. L. Zhao, Z. Hu, C.-Y. Kuo, T.-W. Pi, M.-K. Wu, L. H. Tjeng and A. C. Komarek, *Phys. Status Solidi RRL*, 2015, **9**, 730-734.
57. S. Ivanov, P. Nordblad, R. Mathieu, R. Tellgren, E. Politova and G. André, *Eur. J. Inorg. Chem.*, 2011, **2011**, 4691-4699.

58. N. D. Todorov, M. V. Abrashev, S. C. Russev, V. Marinova, R. P. Nikolova and B. L. Shivachev, *Phys. Rev. B*, 2012, **85**, 214301.
59. G. V. Bazuev, B. G. Golovkin, V. G. Zubkov and A. S. Tyutyunnik, *J. Solid State Chem.*, 1994, **113**, 132-137.
60. R. Becker and H. Berger, *Acta Crystallogr. Sec. E*, 2006, **62**, i261-i262.
61. B. Wedel, I. Kimio and K. Sugiyama, *Z. Kristallogr. NCS*, 2001, **216**, 345.
62. L. Falck, O. Lindqvist and J. Moret, *Acta Crystallogr. Sec. B*, 1978, **34**, 896-897.
63. M. Herak, H. Berger, M. Prester, M. Miljak, I. Živković, O. Milat, D. Drobac, S. Popović and O. Zaharko, *J.Phy.: Condens. Matter*, 2005, **17**, 7667.
64. K. Y. Choi, P. Lemmens, E. S. Choi and H. Berger, *J. Phy.: Condens. Matter*, 2008, **20**, 505214.
65. H. M, *Solid State Commun.*, 2011, **151**, 1588-1592.
66. G. Kaleva, E. Politova, S. Ivanov, A. Mosunov, S. Stefanovich, N. Sadovskaya, R. Mathieu and P. Nordblad, *Inorg. Mater.*, 2011, **47**, 1132-1140.
67. M. Månsson, K. Prša, J. Sugiyama, D. Andreica, H. Luetkens and H. Berger, *Phys. Procedia*, 2012, **30**, 142-145.
68. Z. He and M. Itoh, *J. Magn. Magn. Mater.*, 2014, **354**, 146-150.
69. X. Zhu, Z. Wang, X. Su and P. M. Vilarinho, *ACS Appl. Mater. Inter.*, 2014, **6**, 11326-11332.
70. G. Caimi, L. Degiorgi, H. Berger and L. Forró, *Europhys. Lett.*, 2006, **75**, 496.
71. C. de la Calle, M. J. Martínez-Lope, V. Pomjakushin, F. Porcher and J. A. Alonso, *Solid State Commun.*, 2012, **152**, 95-99.
72. M. Weil, *Z. Anorg. Allg. Chem.*, 2003, **629**, 653-657.
73. R. Becker, M. Johnsson and H. Berger, *Acta Crystallogr. Sec. C*, 2006, **62**, i67-i69.
74. H. Singh, A. K. Sinha, H. Ghosh, M. N. Singh and A. Upadhyay, *AIP Conf. Proc.*, 2015, **1665**, 060021.
75. H. Singh, H. Ghosh, T. V. Chandrasekhar Rao, G. Sharma, J. Saha and S. Patnaik, *J. Appl. Phys.*, 2016, **119**, 044104.
76. H. Singh, H. Ghosh, T. V. Chandrasekhar Rao, A. K. Sinha and P. Rajput, *J. Appl. Phys.*, 2014, **116**, 214106-214101-214106-214107.
77. A. B. Harris, *Phys. Rev. B*, 2012, **85**, 100403.
78. J. L. Her, C. C. Chou, Y. H. Matsuda, K. Kindo, H. Berger, K. F. Tseng, C. W. Wang, W. H. Li and H. D. Yang, *Phys. Rev. B*, 2011, **84**, 235123.
79. W.-H. Li, C.-W. Wang, D. Hsu, C.-H. Lee, C.-M. Wu, C.-C. Chou, H.-D. Yang, Y. Zhao, S. Chang, J. W. Lynn and H. Berger, *Phys. Rev. B*, 2012, **85**, 094431.
80. P. Tolédano, V. Carolus, M. Hudl, T. Lottermoser, D. D. Khalyavin, S. A. Ivanov and M. Fiebig, *Phys. Rev. B*, 2012, **85**, 214439.
81. C.-W. Wang, C.-H. Lee, C.-Y. Li, C.-M. Wu, W.-H. Li, C.-C. Chou, H.-D. Yang, J. W. Lynn, Q. Huang, A. B. Harris and H. Berger, *Phys. Rev. B*, 2013, **88**, 184427.
82. M. Weil, *Acta Crystallogr. Sec. E*, 2006, **62**, i246-i247.